Low doses of Perampanel protect striatal and hippocampal neurons against *in vitro* ischemia by reversing the ischemia-induced alteration of AMPA receptor subunit composition

Petra Mazzocchetti[1], Andrea Mancini[1], Miriam Sciaccaluga[1], Alfredo Megaro[1], Laura Bellingacci[1], Massimiliano Di Filippo[1], Elena Nardi Cesarini[1], Michele Romoli[1], Nicolò Carrano[2], Fabrizio Gardoni[2], Alessandro Tozzi[3,4], Paolo Calabresi[1,3], Cinzia Costa[1]

[1] Neurological Clinic, Department of Medicine, Hospital Santa Maria Della Misericordia, University of Perugia, Perugia, Italy;

[2] Department of Pharmacological and Biomolecular Sciences, University of Milan, Milan, Italy;

[3] Laboratory of Neurophysiology, Santa Lucia Foundation, IRCCS, Rome, Italy;

[4] Department of Experimental Medicine, Section of Physiology and Biochemistry, University of Perugia, Perugia, Italy.

Corresponding author:

Cinzia Costa MD, PhD
Università di Perugia, Clinica Neurologica
Ospedale S. Maria della Misericordia,
S. Andrea delle Fratte, 06156, Perugia - Italy
Tel +39-0755784228
Fax +39-0755784229
Email cinzia.costa@unipg.it

Abstract

Energy depletion caused by ischemic brain insults may result in persistent neuronal depolarization accompanied by hyper-stimulation of ionotropic glutamate receptors and excitotoxic phenomena, possibly leading to cell death. Thus, the use of glutamate receptor antagonists, such as the AMPARs antagonist Perampanel (PER), might be a pharmacological approach to counteract the excessive over-activation of glutamate receptors providing neuroprotective effects. Using electrophysiological and molecular analyses, we investigated the effect of PER against *in vitro* ischemia obtained by oxygen and glucose deprivation (OGD) in rat slices of two brain structures particularly sensitive to ischemic insults, the nucleus striatum and the hippocampus. We found that in these regions, while PER reduced the excitatory synaptic transmission without altering the electric membrane excitability, it was neuroprotective against OGD at doses that did not affect physiological long-term potentiation (LTP). Furthermore, in both the analysed regions, PER blocked the pathological form of LTP, namely ischemic LTP (iLTP). Finally, we proved that the neuroprotective effect of PER against OGD was due to its capability to normalize the subunit synaptic localization and function of AMPAR altered after an ischemic insult. Taken together these findings support the idea that PER is a drug potentially effective to counteract *in vivo* ischemic damage.

Keywords: Neuroprotection, oxygen and glucose deprivation, GluA1 AMPA receptor subunit, ischemic LTP, striatum, hippocampus

Introduction

Energy depletion, caused by reduced blood flow to the central nervous system (CNS), is responsible for diminished supplement of oxygen, glucose and other substances to neurons leading to persistent neuronal depolarization accompanied by increased glutamate release in the extracellular space (Dirnagl et al., 1999).

The subsequent activation of synaptic and non-synaptic glutamate receptors has been suggested to initiate excitotoxic cascades representing a major key pathogenic event in ischemic neuronal death (Bano and Nicotera, 2007; Kwak and Weiss, 2006; Lai et al., 2014; Lipton, 1999).

N-methyl-d aspartic receptors (NMDARs) and α-amino-3-hydroxy-5methyl-4-isoxazole propionate receptors (AMPARs) seem to be strongly implicated in the ischemic-related excitotoxic pathway. In fact, many studies reported that after an ischemic insult these receptors display altered expression and function (Arundine and Tymianski, 2004; Lea and Faden, 2001). The ischemic insult leads to increased GluA1/GluA2 AMPAR subunit ratio, which allows massive Ca^{2+} entry through the receptor (Pellegrini-Giampietro et al., 1997). The AMPAR has also a crucial role in the induction and maintenance of the long-term potentiation (LTP) and long-term depression (LTD), two forms of synaptic plasticity that are thought to represent the basis of memory and learning processes (Buonarati et al., 2019; Malinow and Malenka, 2002). LTP requires changes in the number and function of glutamate receptors, including the synthesis and the insertion in the postsynaptic membrane of new AMPARs to ease the potentiation of synaptic transmission (Buonarati et al., 2019). The relation occurring among ischemic insult, change of glutamate neurotransmission and synaptic plasticity is suggested by the evidence that a brief oxygen and glucose deprivation (OGD) is able to induce a pathological form of synaptic plasticity named ischemic long-term potentiation (iLTP) (Calabresi et al., 2002). This aberrant form of synaptic plasticity has been considered the electrophysiological correlate of the molecular alterations taking place during apoptotic cell death, with still unknown functional consequences (Calabresi et al., 2003). Thus, during pathological conditions characterized by limited neuronal energetic supply, the consequent altered neuronal

synaptic plastic properties could negatively impair the cognitive abilities (Delcasso et al., 2014) and brain coping strategies of patients. A hypothetical optimal neuroprotective strategy for brain ischemia treatment should counteract the activation of the glutamate-triggered excitotoxic pathways without impairing the capability of neurons to express physiological synaptic plasticity. Several glutamate receptors antagonists have been tested as neuroprotective compounds against brain ischemia (Hanada et al., 2011). AMPARs antagonist such as Talampanel and other non-competitive AMPA antagonists have also been considered since these drugs are able to attenuate brain damage after focal or cerebral ischemia (Meldrum and Rogawski, 2007). However, the use of AMPAR antagonists for clinical use also present important limitations since they exhibit many short-comings, such as poor solubility, a short half-life, and precipitation in the kidney (Hanada et al., 2011).

Perampanel (PER) is a AMPARs antagonist, unique for its capability to cross the blood brain barrier respect to other AMPAR antagonists, for showing a good oral bioavailability and favourable pharmacokinetic properties (Rogawski and Hanada, 2013). Thus, due to these properties and the mechanism of action antagonizing glutamate transmission, it is possible to hypothesize a beneficial neuroprotective effect of PER against energetic failure that will preserve neuronal transmission. Following this hypothesis, we analysed the potential neuroprotective effect of PER in the nucleus striatum and in the hippocampus, two brain structures particularly vulnerable to ischemic insults and of pivotal importance for different forms of learning and memory. Furthermore, we tested whether the doses of PER exerting neuroprotective effects against OGD were able to influence the expression of synaptic plasticity as well as the postsynaptic localization of AMPA receptor subunits in both analysed regions.

Materials and methods

All experiments were conducted in conformity with the European Communities Council Directive of November 1986 (86/609/ECC), in accordance with a protocol approved by the Animal Care and

Use Committee at the University of Perugia and with the ARRIVE guidelines. All efforts were made to minimize the number of animals used and their suffering.

Electrophysiology

Corticostriatal and hippocampal slices (thickness 270 and 400 μm respectively) were cut from brains of four weeks old Wistar male rats (Charles River, Italy) using a vibratome. All slices were submerged in an artificial cerebrospinal fluid (ACFS) or Kreb's solution, bubbled with 95% O_2, 5% CO_2 gas mixture at 32°C for cortical striatal slices and 29°C for hippocampal slices (flow rate 2.9-3.3 ml/min). The composition of the Kreb's solution was (in mmol/L) 126 NaCl, 2.5 KCl, 1.2 $MgCl_2$, 1.2 NaH_2PO_4, 2.4 $CaCl_2$, 10 Glucose and 25 $NaHCO_3$. Each single striatal and hippocampal slice was transferred to a recording chamber and submerged in a continuously flowing Kreb's solution for both extracellular and patch-clamp recordings. For extracellular recordings an Axoclamp 2B amplifier (Molecular Devices, USA) was used.

Hippocampal extracellular *excitatory post-synaptic potentials* (fEPSPs) were evoked with a stimulating bipolar electrode placed in the Schaffer collateral fibers (10ms duration; 30-50 V intensity) and recorded with a glass microelectrode filled with 2 mol/L NaCl placed in the *stratum radiatum* of the CA1 hippocampal region. Striatal fEPSPs were evoked every 10 s by stimulating the cortical glutamatergic afferents to the dorsolateral striatum.

In vitro ischemia was delivered by switching the standard Kreb's solution to an artificial cerebrospinal fluid solution gassed with 95% N_2 and 5% CO_2 (oxygen and glucose deprivation, OGD) in which sucrose replaces glucose. The duration of OGD protocol was region specific, 10 min for the striatum and 8 min for the CA1 hippocampal region (Mazzocchetti et al., 2018).

To induce LTP in the CA1 hippocampal region, a high-frequency stimulation (HFS) protocol consisting of one train lasting 1 s, was delivered at 100 Hz (Kleschevnikov et al., 2004) after acquiring a stable baseline for 10 minutes. In hippocampal slices, iLTP was induced by a brief OGD episode (2-2.5 minutes) (Crepel et al., 1993). In these experiments, fEPSPs were evoked in presence

of a Kreb's solution containing 10 μM bicuculline to block $GABA_A$ receptors, 0.3 mM Mg^{2+} to enhance NMDA receptor-mediated response and 10 μM glycine to saturate the glycine allosteric site of the NMDA receptors (Crepel and Ben-Ari, 1996; Crepel et al., 1993).

Whole-cell voltage-clamp recordings (access resistance 15-30MΩ; holding potential -80 mV/-60mV) were performed on striatal spiny projection neurons (SPNs) and pyramidal cells visualized using differential interference contrast (Nomarski) and infrared microscopy (Olympus). Recordings were made with a Multiclamp 700B amplifier (Molecular Devices), using a borosilicate glass pipette (4-7MΩ) filled with a standard internal solution contained (in mM): 145 K^+-gluconate, 0.1 $CaCl_2$, 2 $MgCl_2$, 0.1 EGTA, 10 HEPES, 0.3 Na^+-GTP and 2 Mg^{2+}-ATP, adjusted to pH 7.3 with KOH.

In order to evoked postsynaptic excitatory currents (EPSCs) from SPNs and pyramidal cell a bipolar stimulating electrode were placed intrastriatal or on Schaffer collateral fibers, respectively. Current-voltage (I-V) relationship of both CA1 pyramidal cells and in SPNs was obtained by applying hyperpolarizing and depolarizing steps of current (50 pA, 2 sec). All the experiments were conducted in the presence of 50μM of GABA receptor antagonist picrotoxin, in order to isolate the glutamate transmission.

In the striatum, LTP was induced by HFS protocol consisting of three trains lasting 3 s (20 s interval) delivered at 100 Hz. During HFS protocol, the stimulus intensity was increased to supra-threshold levels. External Mg^{2+} ions were omitted to maximize the contribution of NMDA receptors during LTP experiments (Calabresi et al., 1992).

The iLTP was induced in corticostriatal slices by a brief OGD episode (2-2.5 minutes). Also in this case, external Mg^{2+} ions were omitted to maximize the contribution of NMDA receptors during LTP experiments (Calabresi et al., 1992) and the SPNs were clamped to a holding potential of -50 mV.

Subcellular fractionation and western blotting

For the purification of triton-insoluble postsynaptic fractions (TIF), striatal and hippocampal were homogenized with a Teflon-glass potter in ice-cold buffer containing (in mM) 320 sucrose, 1 Hepes, 1 $MgCl_2$, 1 $NaHCO_3$, 0.1 phenylmethylsulfonylfluoride at pH 7.4 in the presence of Complete™ Protease Inhibitor Cocktail Tablets (Roche Diagnostics, Basel, Switzerland) and phosSTOP™ Phosphatase Inhibitor (Roche Diagnostics). The sample was spun at 13.000 g x 15 minutes at 4°C. The resulting pellet was resuspended in Triton-KCl buffer (0.5% Triton X-100 and 150 mM KCl) and, after 15 minutes incubation on ice, it was spun further at 100.000 g x 1 hour at 4°C. The pellet (triton-insoluble postsynaptic fraction, TIF) was resuspended in 20 mM Hepes buffer supplemented with Complete™ Protease Inhibitor Cocktail Tablets and stored at -80°C.

The levels of AMPAR subunits in the homogenate and TIF were analysed by western blotting. Homogenate and TIF samples were separated onto a 7% acrylamide/bis acrylamide gel. Proteins were blotted onto a nitrocellulose membrane (Bio-Rad, Hercules, CA, USA) and probed with the appropriate primary antibodies followed by the corresponding HRP-conjugated secondary antibodies. Labeling detection was performed with ChemiDoc MP Imaging System (Bio-Rad) and images were acquired with ImageLab software (Bio-Rad). The primary antibodies used in this study are anti-GluA1 (dilution 1:1000; Neuromab), anti-GluA2 (dilution 1:500; Neuromab), anti-GluA3 (dilution 1:1000; Synaptic System), anti-GluA1p845 (dilution 1:1000; Merck Millipore) and anti-tubulin (dilution 1:20000; Sigma-Aldrich). The latter was always used as loading control for normalization.

Drugs

Drugs were bath applied by dissolving them to the desired final concentration in the Krebs' solution and by switching the perfusion from control solution to drug-containing solution. PER was kindly provided by EISAI. In order to evaluate the effect of PER on I-V relationship and synaptic transmission, PER was applied in the recording chamber for at least 20 minutes. In OGD experiments PER was delivered on the recording chamber for at least 10 minutes before OGD and

maintained throughout the experiment. During the HFS protocol, PER was maintained throughout all the duration of the recording.

Statistical analysis

For electrophysiological experiments data analysis was performed off-line using Clampfit 10 (Molecular Devices). Values given in the text and figures are mean ± SEM, n representing the number experiments. Changes of the fEPSP amplitude and slope are expressed as percentage of the baseline, the latter representing the normalized fEPSP or EPSC mean amplitude acquired during a stable period (10-15 minutes) before the start of the experimental protocols involving PER, OGD and HFS. Two-way ANOVA or the Student's t-test was used. For the molecular analysis data were normalized against tubulin and shown in the graph as mean ± SEM. The one-way ANOVA or the Student's t-test was used.

The significance level was established at *$p < 0.05$, **$p<0.01$, ***$p<0.001$.

Results

Effect of PER on synaptic transmission

We tested the effects of PER on the excitatory synaptic transmission by extracellular field potentials recordings of the CA1 hippocampal region and dorsal striatum stimulating respectively the Schaffer's collaterals or the corticostriatal glutamatergic fibers. After acquiring stable fEPSPs responses for 10 minutes, PER was bath applied for 20 minutes on the slice at different concentrations (striatum 0.1 nM to 1000 nM, hippocampus 1 nM to 3000 nM, Fig. 1A, B). As expected, PER dose-dependently reduced the fEPSP response in both striatum and hippocampus. Specifically, we found that in striatal slices, while 0.1-0.3 nM PER did not reduce the fEPSP amplitude, doses higher than 1 nM were effective, (PER 3 nM, fEPSP amplitude 87.51 ± 2.27%, control vs 1 nM PER (n=12) Student's t-test, $p<0.01$, Fig. 1A). The calculated IC_{50} for the dose-response relationship was 132 nM.

In the hippocampus PER doses lower than 100 nM were unable to reduce the fEPSP slope. In fact, while 1-30 nM PER did not affect the response, in the presence of 100 nM PER the fEPSP slope was 80.49 ± 3.10 % of the baseline (control vs PER, (n=5) Student's t-test, $p<0.05$, Fig. 1B). In the CA1 hippocampal region, PER induced a dose-dependent reduction of the fEPSP slope with an IC_{50} of 355 nM (Fig. 1B).

Effect of PER on the OGD-induced loss of the field potential

We then analysed the possible neuroprotective effect of PER against neuronal damage induced by *in vitro* ischemia (OGD) in the nucleus striatum. After recording in striatal slices a stable fEPSP for 10 minutes, an oxygen and glucose-free solution was applied for 10 minutes, a time known to produce the irreversible loss of the fEPSP amplitude in this region (Calabresi et al., 2000). The fEPSP amplitude was recorded for additional 30 minutes both in control experiments or in the presence of different concentrations of PER. We found that, the ischemic insult irreversibly suppressed the fEPSP both in control conditions and in the presence of 0.1 nM PER (control (n=7) vs PER (n=6), two-way ANOVA, $p>0.05$; Fig. 2A). Conversely, 0.3 nM and 1 nM PER were able to induce a significant recovery of the fEPSP amplitude, as measured 30 minutes following OGD (PER 0.3 nM fEPSP amplitude 78.72 ± 8.17% of baseline, control (n=7) vs PER (n=7), two-way ANOVA, $p<0.001$; PER 1 nM fEPSP amplitude 85.44 ± 11.55% of baseline, control (n=7) vs PER (n=6), two-way ANOVA, $p<0.001$; Fig. 2B, C). These data indicate that, in the nucleus striatum, the neuroprotective effect of PER against *in vitro* ischemia is dose-dependent presenting a maximal neuroprotective effect achieved by 1 nM of the drug and a calculated EC_{50} of 0.16 nM (Fig. 2D). In order to test whether the first dose of PER that was able to protect neurons against *in vitro* ischemia could affect the membrane excitability of SPNs, we performed whole-cell patch-clamp recordings of striatal SPNs to measure the firing activity before and 10 minutes after exposure of the slices to 0.3 nM (Fig. 2E). The calculated I-V curves showed no differences between the recordings obtained

in control conditions and in the presence of 0.3 nM PER for the striatum (striatum, control vs 0.3 nM PER (n=5), two-way ANOVA, $p>0.05$).

Since the CA1 hippocampal region is one of the most vulnerable areas of the brain to ischemia (Pulsinelli, 1985), 8 minutes OGD are sufficient to produce the irreversible depression of synaptic activity. We found that, in the hippocampal CA1 region, the ischemic insult irreversibly suppressed the fEPSP both in control experiments and in the presence of 10 nM PER (control (n=7) vs PER (n=5), two-way ANOVA, $p>0.05$, Fig. 3A). Conversely, 30 and 100 nM PER significantly recovered the fEPSP, as measured 30 minutes after the OGD application (PER 30 nM, fEPSP slope 53.53 ± 9.63% of baseline, control (n=7) vs PER (n=6), two-way ANOVA, $p<0.001$, Fig. 3B; PER 100 nM, fEPSP slope 98.87 ± 5.69% of baseline control (n=7) vs PER (n=5), two-way ANOVA, $p<0.001$, Fig. 3C). Interestingly, 100 nM PER caused only a mild reduction of excitatory synaptic transmission (Fig. 1B). The neuroprotective effect of PER was dose-dependent with a calculated EC_{50} of 30.04 nM (Fig. 3D). The calculated I-V curves showed no differences between the recordings obtained in control conditions and in the presence of 30 nM PER of hippocampal CA1 pyramidal neurons (control vs 30 nM PER (n=4), two-way ANOVA, $p>0.05$; Fig. 3E).

Effect of PER on physiological and ischemic long-term potentiation of synaptic transmission

AEDs are known to possibly induce memory deficits in patients, even at therapeutic doses, as confirmed also in experimental models (Detrait et al., 2010). Thus, we tested whether PER neuroprotective doses against OGD impaired LTP induction both in the nucleus striatum and hippocampus. To achieve this goal, we recorded striatal EPSCs for SPNs and fEPSPs for pyramidal cells, for 10 minutes and induced LTP by HFS of afferent fibres to the striatum or to the CA1 hippocampal region. The EPSCs amplitude measured 30 minutes after the HFS protocol in the striatum and the fEPSP slopes measured 50 minutes after the HFS in the hippocampus were not significantly different in control experiments and in the presence of PER in both the structures (striatum, EPSCs amplitude in control conditions 158.48 ± 6.16%, in PER 0.3 nM 144.10 ±

11.31%, control (n=5) vs PER (n=5), two-way ANOVA, $p>0.05$; Fig. 4A; hippocampus, fEPSP slope in control conditions, 167.76 ± 16.56%, in 30 nM PER, 139.92 ± 9.28%, control (n=5) vs PER (n=5), two-way ANOVA, $p>0.05$, Fig. 4B). It should be noted that in the CA1 hippocampal region 100 nM PER, the dose producing maximal neuroprotective effect, significantly impaired the LTP (data not shown).

We next tested the effects of PER on iLTP, an aberrant form of synaptic plasticity reflecting metabolic neuronal suffering induced by an ischemic insult. In the nucleus striatum, a brief OGD episode (2-2.5 minutes) is able to induce a transient depression of the EPSCs of SPNs followed, after washout of the ischemic solution, by reversal of the phenomenon and a subsequent and persistent potentiation of the EPSCs amplitude (EPSCs amplitude 30 minutes after OGD 155.15 ± 4.28% of baseline; Fig. 4 C). We found that the application of 0.3 nM PER prevented the occurrence of iLTP (EPSCs amplitude 85.77 ± 7.78%, control (n=4) vs PER (n= 4), $p<0.001$, Fig. 4C). As previously shown (Costa et al., 2011), in the hippocampus OGD was also able to induce iLTP (fEPSPs slope 30 minutes after OGD 140.91 ± 1.90% of baseline) and interestingly, 30 nM PER was able to prevent the induction of the pathological LTP in this region (PER, fEPSPs slope 30 minutes after OGD 98.37 ± 6.82% of baseline; control (n=6), vs PER 30 nM (n=5), $p<0.001$, Fig. 4D).

Effect of PER on OGD-induced alterations of AMPA receptor subunit composition

We evaluated by western blotting analysis in a total homogenate fraction and in a triton-insoluble post-synaptic fraction (TIF), the possibility that alterations in the levels and subunit composition of AMPA may be involved in the observed effects induced by OGD and treatment with PER. Analysis of AMPAR subunit levels in total homogenate indicated a higher expression both GluA1 and GluA2 subunits in the hippocampus compared to the striatum ($p<0.01$, GluA1, hippocampus *vs* striatum; $p<0.05$, GluA2, hippocampus *vs* striatum; Fig. 5A).

Moreover, we found that application of the OGD protocol to hippocampal slices induced a significant increase of GluA1 AMPAR subunit synaptic levels (*p<0.05, post-OGD *vs* pre-OGD, Fig. 5B). Notably, concomitant treatment with PER was sufficient to rescue synaptic GluA1 subunit to control levels (#p<0.05, post-OGD + PER *vs* post-OGD, Fig. 5B). Similarly, PER significantly decreased GluA1 synaptic levels in the striatum from OGD-treated corticostriatal slices (#p<0.05, post-OGD + PER *vs* post-OGD, Fig. 5C). No effect on GluA2 and GluA3 subunit levels at synapses was observed after OGD in absence or presence of PER both in hippocampus (Fig. 5B) and in striatum (Fig. 5C). Finally, no alteration of the phosphorylation of GluA1-Ser845, a well-validated marker of synaptic plasticity (Esteban et al., 2003; Hu et al., 2007; Oh et al., 2006), was found both in hippocampus (Fig. 5B) and in striatum (Fig. 5C).

Discussion

In this study we explored the possible neuroprotective effect of the AMPAR antagonist PER on energy deprivation induced by bath application of an oxygen- and glucose-free solution (OGD) on rat hippocampal and striatal slices. We found that PER, at doses unable to affect neurotransmission and the physiological LTP, was able to reduce the detrimental effects of OGD on hippocampal and striatal neurons, including the expression of iLTP, a pathological form of synaptic plasticity. Finally, we proved that PER exerted this neuroprotective effect through the reduction of GluA1-bearing AMPARs that was increased during OGD.

We found that in the nucleus striatum and in the hippocampus the AMPARs antagonist PER at higher concentrations (higher than 30 nM in the striatum, higher 100 nM in the hippocampus) reduces synaptic transmission in a concentration-dependent manner, as previously described (Ceolin et al., 2012). We found that the IC_{50} of PER in the striatum (132 nM) was significantly lower than that measured in the hippocampus (355 nM), highlighting the higher sensitivity of the striatum to the drug in respect to the hippocampus. This difference could be explained by the

different expression of AMPARs in these brain regions, as observed by molecular analysis of AMPARs subunit levels in total homogenate of these tissues.

Moreover, we found that PER exerted, a dose-dependent, neuroprotective effect also against *in vitro* ischemia obtained by OGD, and it was able to block the pathological iLTP in both the striatum and hippocampus. In fact, AMPARs are known to be particularly important for striatal (Di Filippo et al., 2008; Saulle et al., 2002) and hippocampal iLTP (Dias et al., 2013).

It is worth noting that the neuroprotective effect of PER was achieved at very low concentrations, respect to that required for antiepileptic action (Biton, 2007; Costa et al., 2011). Similarly, the antiepileptic drug (AED) Zonisamide had also neuroprotective effects against iLTP at doses lower than that used as anticonvulsant (Costa et al., 2011).

A possible explanation of this neuroprotective effect could rely on the changes of AMPARs subunit composition induced by ischemic insult (Dos-Anjos et al., 2009), influencing the synaptic susceptibility to PER. In fact, we found that OGD selectively increased the number of AMPARs expressing the GluA1 subunit, which possibly leads to the presence at synapses of novel GluA2-lacking Ca^{2+} AMPARs. PER seems to act specifically on GluA1 subunit thus it might be possible that it is able to protect neurons at doses lower than that affecting synaptic transmission, due to the high expression of GluA1 subunit after OGD in contrast to physiological conditions, in which the high majority of AMPARs express a GluA1/GluA2 or GluA2/GluA3 configuration. Indeed, PER neuroprotective effect might be related to the selective block of GluA1 subunit, rescuing physiological Ca^{2+}-impermeable AMPARs at synaptic level after an ischemic insult and preventing the harmful increase of intracellular Ca^{2+} leading to neuronal death. Moreover, the observation that PER-dependent neuroprotective effects were achieved at doses not significantly influencing basal excitatory transmission could also suggest that the PER-dependent beneficial effect acted through non-synaptic AMPA receptors or, more intriguingly, additionally unveiled neuroprotective pathways.

Interestingly, in support of the neuroprotective use of PER, it has been demonstrated that this drug was able to ameliorate the post-stroke motor function and the spatial working memory in a rat model of transient middle cerebral artery occlusion (MCAO) through possible anti-inflammatory and antioxidant mechanisms (Nakajima et al., 2018). Moreover, PER has been reported to reduce brain oedema, brain infarct volume and neuronal apoptosis following focal cerebral ischemia in rats (Niu et al., 2018). Unlike other compounds affecting AMPAR function such as NBQX or Talampanel which exhibit many shortcomings (Hanada et al., 2011; Langan et al., 2003), PER present good oral bioavailability and favourable pharmacokinetic properties (Rogawski and Hanada, 2013) making it a good candidate for post-stroke neuroprotective strategy.

Although many AEDs, such as PER, present potential neuroprotective effect, they are known to exert negative dose-dependent effects on cognitive functions (Helmstaedter and Witt, 2013; Witt et al., 2015). In fact, they have been shown to affect cognition in adult human subjects (Sgobio et al., 2010) and to affect morphogenesis and brain development by influencing synaptogenesis, synaptic plasticity and neural network formation (Caccamo et al., 2016; Ikonomidou and Turski, 2010). Accordingly, phenytoin can induce brain atrophy in patients after long-term use (Ney et al., 1994), while valproic acid may produce morphologic alterations and impairment of specific hippocampal-dependent memory tasks (Sgobio et al., 2010). For this reason, the evaluation of the effects of AEDs on synaptic plasticity and cognition is critical.

Thus, we evaluated whether PER, at doses able to protect neurons from OGD, also affected the physiological expression of LTP in hippocampal and striatal areas. Our results suggest that the dose of PER exerting neuroprotective effect against *in vitro* ischemia does not alter LTP of striatal neurons. In CA1 hippocampal region, while 30nM PER is neuroprotective against OGD and LTP is spared, the neuroprotective effect of higher PER doses (100 nM) is associated to impaired LTP. Thus, it is conceivable that PER has a dose-dependent effect on LTP, reflecting its direct effect on synaptic transmission. These preclinical results could justify the clinical data of the literature, where

Witt and colleagues demonstrated a considerable adverse effect of a higher drug load on cognition, especially on executive functions (Witt et al., 2015).

Conclusion

Our results suggest that PER exerts a neuroprotective effect against energy deprivation in two brain regions particularly sensitive to ischemic insult and of fundamental importance in memory processes. A significant protection was reached at concentrations of the drug unable to affect synaptic transmission and plasticity with different efficacy in striatum and hippocampus. Taken together these findings support PER, as a third generation AED, as a good candidate for further investigation for the treatment of brain ischemia.

Acknowledgements section:

We thank EISAI for kindly providing Perampanel.

Financial Disclosures:

This study was supported by EISAI

References

Arundine, M., Tymianski, M., 2004. Molecular mechanisms of glutamate-dependent neurodegeneration in ischemia and traumatic brain injury. Cell Mol Life Sci. 61**,** 657-68.

Bano, D., Nicotera, P., 2007. Ca2+ signals and neuronal death in brain ischemia. Stroke. 38**,** 674-6.

Biton, V., 2007. Clinical pharmacology and mechanism of action of zonisamide. Clin Neuropharmacol. 30**,** 230-40.

Buonarati, O. R., et al., 2019. Mechanisms of postsynaptic localization of AMPA-type glutamate receptors and their regulation during long-term potentiation. Sci Signal. 12.

Caccamo, D., et al., 2016. Neuroprotection as a Potential Therapeutic Perspective in Neurodegenerative Diseases: Focus on Antiepileptic Drugs. Neurochem Res. 41**,** 340-52.

Calabresi, P., et al., 2003. Synaptic plasticity in the ischaemic brain. Lancet Neurol. 2**,** 622-9.

Calabresi, P., et al., 1992. Long-term synaptic depression in the striatum: physiological and pharmacological characterization. J Neurosci. 12**,** 4224-33.

Calabresi, P., et al., 2000. Is pharmacological neuroprotection dependent on reduced glutamate release? Stroke. 31**,** 766-72; discussion 773.

Calabresi, P., et al., 2002. Post-ischaemic long-term synaptic potentiation in the striatum: a putative mechanism for cell type-specific vulnerability. Brain. 125**,** 844-60.

Ceolin, L., et al., 2012. A novel anti-epileptic agent, perampanel, selectively inhibits AMPA receptor-mediated synaptic transmission in the hippocampus. Neurochem Int. 61**,** 517-22.

Costa, C., et al., 2011. A critical role of NO/cGMP/PKG dependent pathway in hippocampal post-ischemic LTP: modulation by zonisamide. Neurobiol Dis. 44**,** 185-91.

Crepel, V., Ben-Ari, Y., 1996. Intracellular injection of a Ca2+ chelator prevents generation of anoxic LTP. J Neurophysiol. 75**,** 770-9.

Crepel, V., et al., 1993. A selective LTP of NMDA receptor-mediated currents induced by anoxia in CA1 hippocampal neurons. J Neurophysiol. 70**,** 2045-55.

Delcasso, S., et al., 2014. Functional relationships between the hippocampus and dorsomedial striatum in learning a visual scene-based memory task in rats. J Neurosci. 34**,** 15534-47.

Detrait, E. R., et al., 2010. Brivaracetam does not alter spatial learning and memory in both normal and amygdala-kindled rats. Epilepsy Res. 91**,** 74-83.

Di Filippo, M., et al., 2008. Plasticity and repair in the post-ischemic brain. Neuropharmacology. 55**,** 353-62.

Dias, R. B., et al., 2013. Ischemia-induced synaptic plasticity drives sustained expression of calcium-permeable AMPA receptors in the hippocampus. Neuropharmacology. 65**,** 114-22.

Dirnagl, U., et al., 1999. Pathobiology of ischaemic stroke: an integrated view. Trends Neurosci. 22**,** 391-7.

Dos-Anjos, S., et al., 2009. Global ischemia-induced modifications in the expression of AMPA receptors and inflammation in rat brain. Brain Res. 1287**,** 20-7.

Esteban, J. A., et al., 2003. PKA phosphorylation of AMPA receptor subunits controls synaptic trafficking underlying plasticity. Nat Neurosci. 6**,** 136-43.

Hanada, T., et al., 2011. Perampanel: a novel, orally active, noncompetitive AMPA-receptor antagonist that reduces seizure activity in rodent models of epilepsy. Epilepsia. 52**,** 1331-40.

Helmstaedter, C., Witt, J. A., 2013. The longer-term cognitive effects of adjunctive antiepileptic treatment with lacosamide in comparison with lamotrigine and topiramate in a naturalistic outpatient setting. Epilepsy Behav. 26**,** 182-7.

Hu, H., et al., 2007. Emotion enhances learning via norepinephrine regulation of AMPA-receptor trafficking. Cell. 131**,** 160-73.

Ikonomidou, C., Turski, L., 2010. Antiepileptic drugs and brain development. Epilepsy Res. 88**,** 11-22.

Kleschevnikov, A. M., et al., 2004. Hippocampal long-term potentiation suppressed by increased inhibition in the Ts65Dn mouse, a genetic model of Down syndrome. J Neurosci. 24**,** 8153-60.

Kwak, S., Weiss, J. H., 2006. Calcium-permeable AMPA channels in neurodegenerative disease and ischemia. Curr Opin Neurobiol. 16**,** 281-7.

Lai, T. W., et al., 2014. Excitotoxicity and stroke: identifying novel targets for neuroprotection. Prog Neurobiol. 115**,** 157-88.

Langan, Y. M., et al., 2003. Talampanel, a new antiepileptic drug: single- and multiple-dose pharmacokinetics and initial 1-week experience in patients with chronic intractable epilepsy. Epilepsia. 44**,** 46-53.

Lea, P. M. t., Faden, A. I., 2001. Traumatic brain injury: developmental differences in glutamate receptor response and the impact on treatment. Ment Retard Dev Disabil Res Rev. 7**,** 235-48.

Lipton, P., 1999. Ischemic cell death in brain neurons. Physiol Rev. 79**,** 1431-568.

Malinow, R., Malenka, R. C., 2002. AMPA receptor trafficking and synaptic plasticity. Annu Rev Neurosci. 25**,** 103-26.

Mazzocchetti, P., et al., 2018. Lacosamide protects striatal and hippocampal neurons from in vitro ischemia without altering physiological synaptic plasticity. Neuropharmacology. 135**,** 424-430.

Meldrum, B. S., Rogawski, M. A., 2007. Molecular targets for antiepileptic drug development. Neurotherapeutics. 4**,** 18-61.

Nakajima, M., et al., 2018. AMPA Receptor Antagonist Perampanel Ameliorates Post-Stroke Functional and Cognitive Impairments. Neuroscience. 386**,** 256-264.

Ney, G. C., et al., 1994. Cerebellar atrophy in patients with long-term phenytoin exposure and epilepsy. Arch Neurol. 51**,** 767-71.

Niu, H. X., et al., 2018. The Orally Active Noncompetitive AMPAR Antagonist Perampanel Attenuates Focal Cerebral Ischemia Injury in Rats. Cell Mol Neurobiol. 38**,** 459-466.

Oh, M. C., et al., 2006. Extrasynaptic membrane trafficking regulated by GluR1 serine 845 phosphorylation primes AMPA receptors for long-term potentiation. J Biol Chem. 281**,** 752-8.

Pellegrini-Giampietro, D. E., et al., 1997. The GluR2 (GluR-B) hypothesis: Ca(2+)-permeable AMPA receptors in neurological disorders. Trends Neurosci. 20**,** 464-70.

Pulsinelli, W. A., 1985. Selective neuronal vulnerability: morphological and molecular characteristics. Prog Brain Res. 63**,** 29-37.

Rogawski, M. A., Hanada, T., 2013. Preclinical pharmacology of perampanel, a selective non-competitive AMPA receptor antagonist. Acta Neurol Scand Suppl. 19-24.

Saulle, E., et al., 2002. Endogenous dopamine amplifies ischemic long-term potentiation via D1 receptors. Stroke. 33**,** 2978-84.

Sgobio, C., et al., 2010. Hippocampal synaptic plasticity, memory, and epilepsy: effects of long-term valproic acid treatment. Biol Psychiatry. 67**,** 567-74.

Witt, J. A., et al., 2015. Adverse cognitive effects of antiepileptic pharmacotherapy: Each additional drug matters. Eur Neuropsychopharmacol. 25**,** 1954-9.

Figure Legends

Figure 1. Effect of PER on physiological synaptic transmission in striatum and CA1 hippocampal region. A) Upper representative traces of striatal fEPSPs recorded in Kreb's solution or in the presence of increasing doses of PER; the graph describes the dose-response curve for PER showing an IC_{50} of 132 nM (control vs 0.1 nM PER (n=7), $p>0.05$; control vs 0.3 nM PER (n=11), $p>0.05$, control vs 3 nM PER (n=8), $p<0.01$; control vs 10 nM PER (n=6), $p<0.05$, control vs 30 nM PER (n=9), $p<0.01$, control vs 300 nM PER (n=6), control vs 1000 nM PER (n=5), $p<0.01$). **B)** Upper representative traces of hippocampal fEPSPs. The graph describes the dose-response curve for PER showing an IC_{50} of 355 nM (control vs 1 nM to 30 nM, (n=5, for each concentration), $p>0.05$; control vs 300 nM PER (n=5), $p<0.01$, control vs 3000 nM PER (n=5), $p<0.001$).

Figure 2. Neuroprotective effect of PER against OGD in striatum. A-C) Upper representative traces of striatal fEPSPs recorded pre and post-OGD both in control condition and in the presence of increasing doses of PER. The time-course plot shows the effect of OGD in control slices and in slices treated with 0.1, 0.3 and 1 nM PER (control open circle; 0.1 nM PER blue circle; 0.3 nM PER (blue square; 1 nM PER blue diamond). **D)** Dose-response curve of the neuroprotective effect of PER on *in vitro* ischemia induced by the OGD in the striatal region. The EC_{50} is 0.16 nM. **E)** Input-Output (I/O) curves recorded from striatal neurons show no difference between neurons recorded in control condition and those treated with PER (striatum, control open circle vs 0.3 nM PER blue circle).

Figure 3. Neuroprotective effect of PER against OGD in CA1 hippocampal region. A-C) Upper representative traces of striatal fEPSPs recorded pre and post-OGD both in control condition and in the presence of increasing doses of PER. The time-course plot shows the effect of OGD in control slices and in slices treated with 10, 30 and 100 nM PER (control open circle; 10 nM PER orange circle; 30 nM PER orange square; 100 nM PER orange diamond). **D)** Dose-response curve of the neuroprotective effect of PER on in vitro ischemia induced by the OGD protocol. The graph

show that the maximal neuroprotective effect was achieved with 100 nM PER. The EC_{50} was 34.21 nM. **E)** Input-Output (I/O) curves recorded from pyramidal neurons show no difference between neurons recorded in control condition and those treated with PER (control open circle vs 30 nM PER orange circle).

Figure 4. Effect of PER on LTP and iLTP in the dorsolateral striatum and in CA1 hippocampal region. A, C) Representative traces of EPSCs recorded before and after the HFS (A) or the OGD protocol (C), in control condition and in the presence of 0.3 nM PER. The time-courses show the EPSCs amplitude before and after the HFS (A) or OGD (C) protocol, in control condition (open circle) and in the presence of 0.3 nM PER (blue circle). **B, D)** Representative traces of fEPSPs recorded before and after the HFS (B) or the OGD (D) protocol, in control condition and in the presence of 30 nM PER (orange circle). Time-course of the fEPSPs amplitude before and after the HFS (B) or OGD (D) protocol, in control condition (open circle) and in the presence of 30 nM PER (orange circle).

Figure 5. Levels of AMPA receptor subunits in hippocampus and striatum in physiological condition, after OGD insult and in the presence of PER. A) WB analysis for GluA1, GluA2 and GluA3 subunits of the AMPARs in the homogenate fraction from striatum and hippocampus. Data are normalized against tubulin and are shown in the graph as mean ± SEM. **p<0.01, *p<0.05. **B-C)** WB analysis for GluA1, GluA1-p845, GluA2 and GluA3 subunits of the AMPARs in the triton insoluble postsynaptic fraction (TIF) from control and OGD-treated corticostriatal and hippocampal slices in absence or presence of PER. Data are normalized against tubulin and are shown in the graph as mean ± SEM. *p<0.05.

Figure 1

Click here to download high resolution image

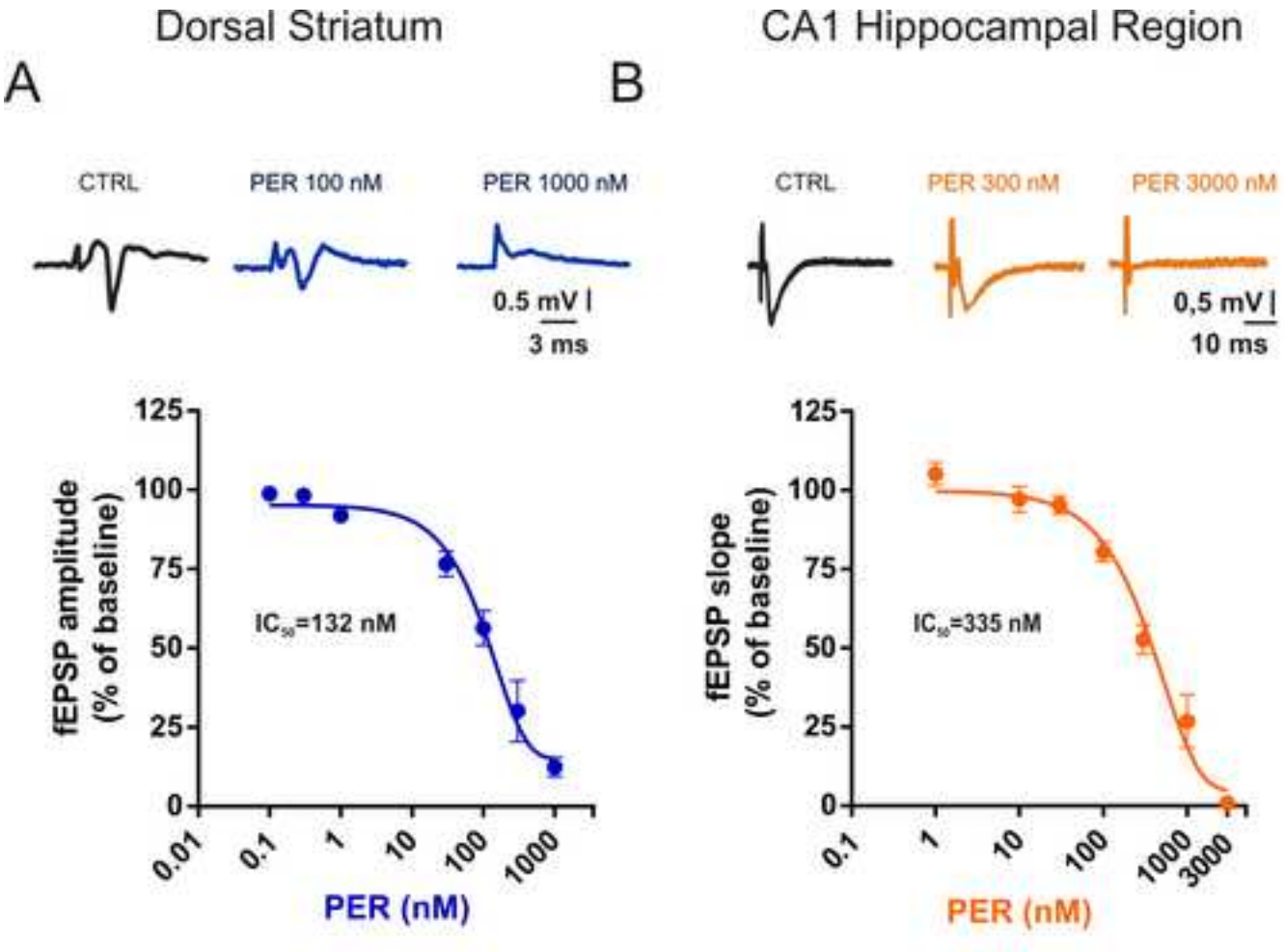

Fig.1

Figure 2

Click here to download high resolution image

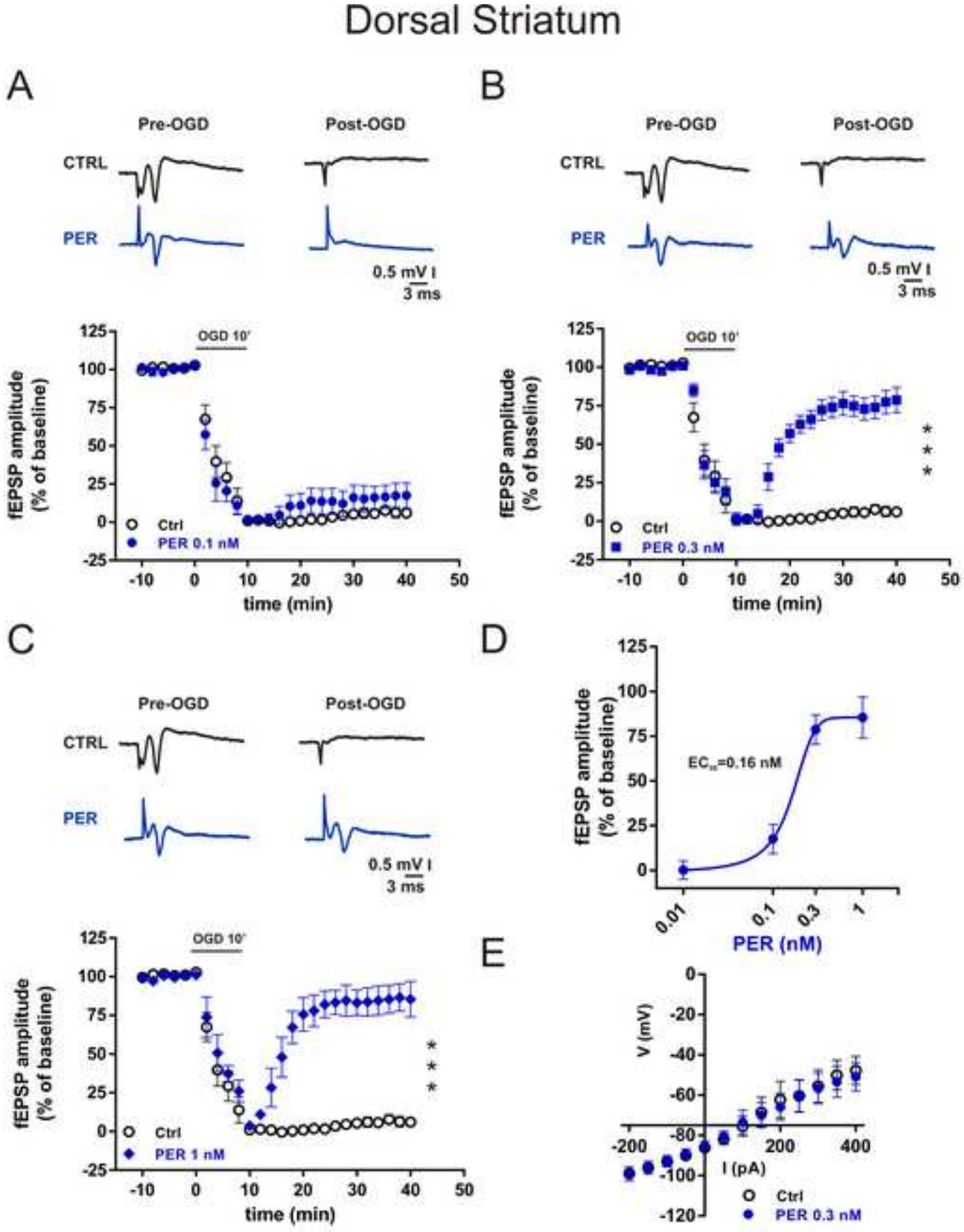

Fig.2

Figure 3

Click here to download high resolution image

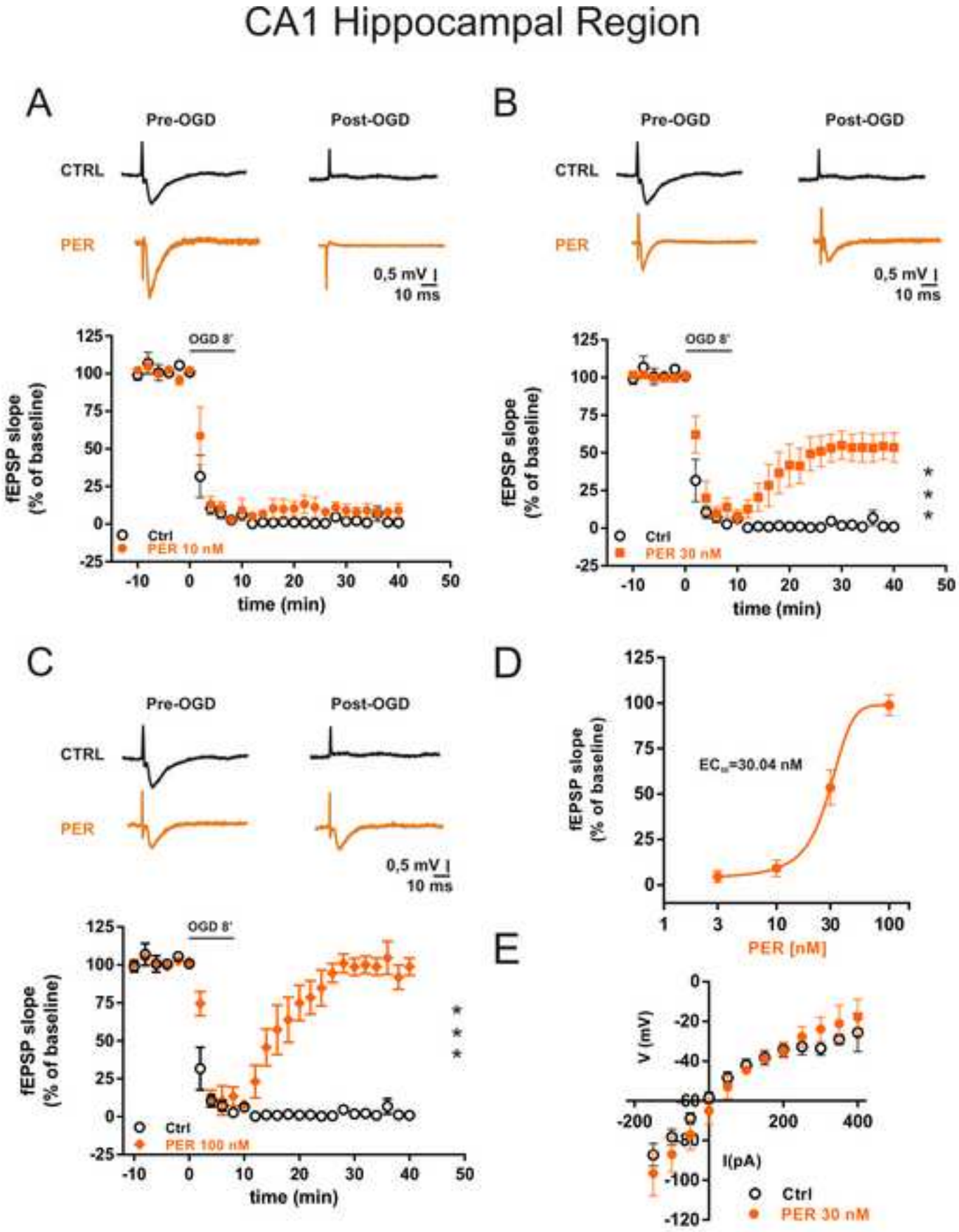

Fig.3

Figure 4

Click here to download high resolution image

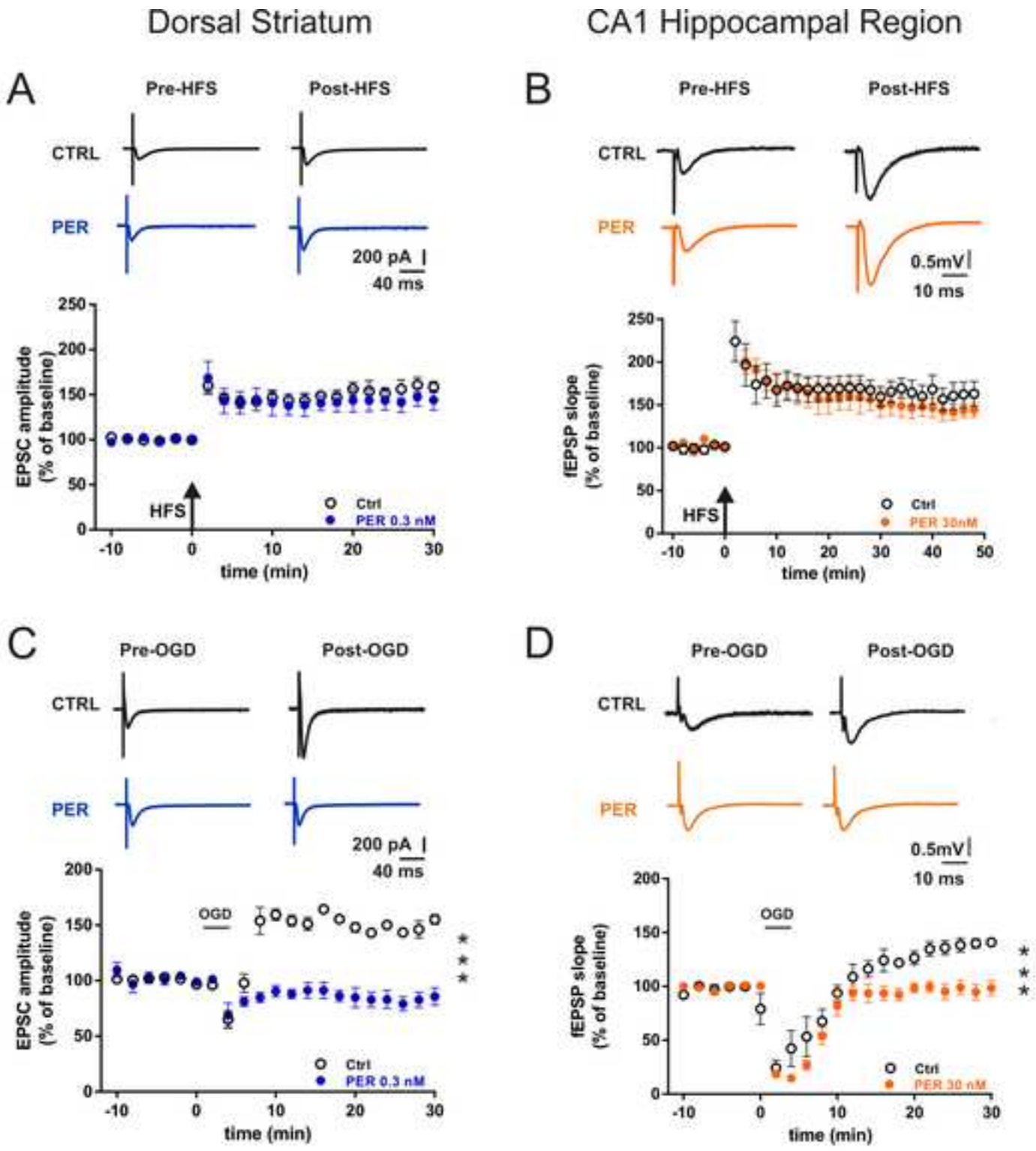

Fig.4

Figure 5

Click here to download high resolution image

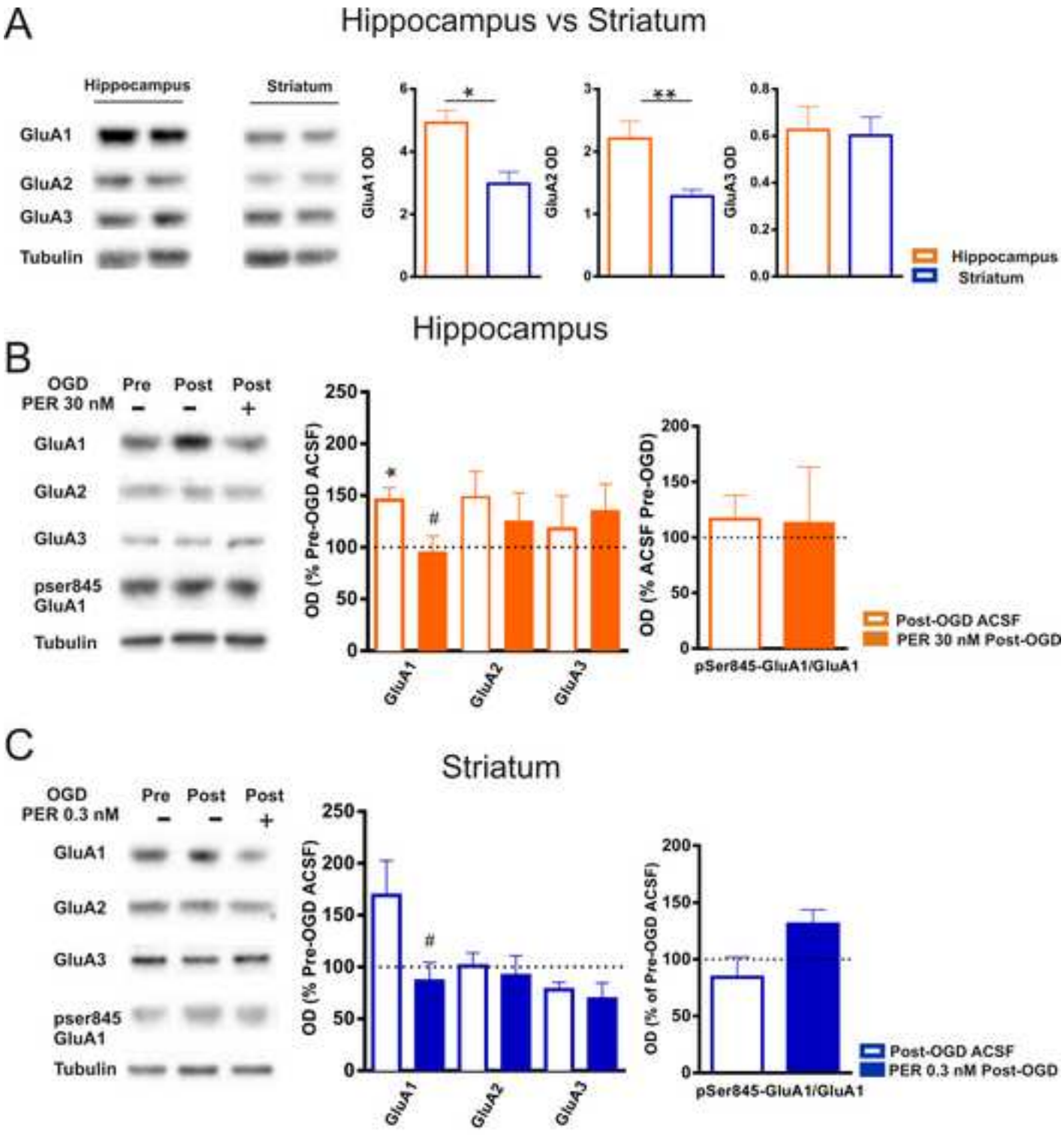

Fig.5